OPEN ACCESS

Original Article

DOI: 10.53389/RJAHS.2025040203

Computational Mapping of Pathogenic Variants in the Fas/Fas Ligand Apoptotic Pathway

Amna Ayub[1], Khulod Ebraheem Hassan [2], Saima Sadaf [3]*

[1,3]Biopharmaceuticals and Biomarkers Discovery Lab., School of Biochemistry and Biotechnology, University of the Punjab, Lahore-54590, Pakistan. [2]Department of Food Science and Quality Control, University of Sulaimani, Iraq.

Author`s Contribution

[AA]performed in-silico studies and analyzed the raw data. [KEH] organized and critically assessed the results. The project conception, overall research supervision and critical review of the draft for intellectual instructions were done by [SS].

Article Info.

Received: Sep 04, 2025
Acceptance: Dec 05, 2025

Conflict of Interest: None

Funding Sources: None

Address of Correspondence

Prof. Dr. Saima Sadaf*
Group Leader, Biopharmaceuticals and Biomarkers Discovery Lab., School of Biochemistry and Biotechnology, University of the Punjab, Lahore, Pakistan.
Email: saima.sbb@pu.edu.pk

ABSTRACT

Background: The Fas receptor (FAS) and its ligand (FASLG) are key regulators of the extrinsic apoptotic pathway, play essential role in immune homeostasis. Their genetic alterations disrupt apoptotic signaling and contribute to autoimmune disorders, and cancer.

Objective: This study was designed to perform a comprehensive *in-silico* analysis to identify pathogenic missense variants in FAS and FASLG and to evaluate their structure-functional consequences.

Methodology: 12 different pathogenicity prediction tools were used to screen 392 missense variants of FAS and structural modeling was performed. Interaction analyses was performed with GeneMANIA and COACH.

Results: We identified G112S (rs2133504146) as the deleterious variant. Consensus filtering initially highlighted 82 risk-associated variants, including C85Y (rs2133502994), C119Y (rs2133513826), and C127G (rs1848386782). Structural modeling confirmed conformational alterations and disulfide bond loss in these variants. Similarly, 258 missense variants in FASLG were analyzed and were narrowed down to 44 high-confidence pathogenic variants. Among these, N184K (rs771262843), N250D (rs1659251672), and N260K (rs761374744) were predicted to abrogate N-glycosylation sites within the TNF homology domain, potentially impairing ligand function. Pathogenic FAS variants were predominantly localized to the extracellular ligand-binding domain, whereas those in FASLG clustered within the TNF homology region.

Conclusion: Collectively, this work delineates key pathogenic variants within the FAS/FASLG axis, provides mechanistic insights into how disrupted apoptosis contributes to immune dysregulation, and sets a foundation for their future experimental validation.

Key words: Autoimmune disorders, Immune homeostasis, Fas receptor, Missense Mutations, Pathogenicity, Computational tools

Introduction

Dysregulation of 'immune homeostasis' is amongst the major contributors to the pathogenesis of autoimmune diseases like rheumatoid arthritis, lymphoproliferative disorders, and malignant tumors. A fundamental mechanism that governs the 'immune equilibrium' is apoptosis or programmed cell death, which helps eliminating the damaged, infected, and autoreactive cells.[1,2] Amongst the major apoptotic pathways, the death receptor–mediated extrinsic pathway is primarily regulated by the Fas receptor (FAS, also called as CD95) and its ligand (FASLG, also known as CD95L). Engagement of Fas-by-Fas ligand induces receptor trimerization, recruitment of FADD and procaspase-8, and formation of death-inducing signaling complex (DISC), that culminates in caspase activation and apoptotic cell death.[3,4]

Structurally, the FAS receptor (encoded by *FAS* gene, located on chromosome 10) is comprised of an extracellular ligand-binding domain and an intracellular death domain. The FASLG gene, located on chromosome 1, encodes Fas ligand, which is primarily expressed in activated T cells and NK cells. Defects in the Fas/FasL signaling pathway may lead to compromised lymphocyte deletion, defective immune surveillance, excessive autoreactivity, and impaired apoptosis.[3,5] Studies have shown that heterozygous FAS mutations are the most frequent cause of autoimmune lymphoproliferative syndrome (ALPS) - a

DOI: 10.53389/RJAHS.2025040203

disorder characterized by splenomegaly, lymphadenopathy, cytopenias, and accumulation of double-negative T cells.[6,7,8]

Initial evidence for the role of Fas signaling in lymphoproliferation emerged from the lpr and gld mouse models, which harbor mutations in Fas and Fasl, respectively. This was followed by the identification of pathogenic FAS mutations in human ALPS, establishing defective Fas-mediated apoptosis as the molecular basis of the disease.[9,10] Many FAS mutations act through haploinsufficiency or dominant-negative mechanisms that interfere with DISC assembly and downstream caspase activation.[11,12]

Genetic variations may emerge through both germline inheritance or somatic mutations, and when present at a frequency of 1% or greater in a population, these are generally classified as polymorphism.[13] Among the different types of genetic variations, nonsynonymous single nucleotide polymorphisms (nsSNPs) are of particular biological importance because they result in amino acid substitutions that can directly affect protein structure, stability, and function. These variants represent one of the most common molecular mechanisms underlying altered protein behavior in human disease.[13,14]

In this study, we have performed comprehensive *in silico* mutational analysis of FAS and FASLG genes to: i) identify high-confidence pathogenic missense variants, ii) assess their effects on protein stability, post-translational modifications, and domain integrity, and iii) define variants most likely to contribute to immune-related disease mechanisms. The findings are interesting uncovering high-risk pathogenic mutations for further experimental validation.

Materials and Methods

FAS and FASLG were selected based on extensive literature review and differential expression data from immune-related disease datasets in the Gene Expression Omnibus (GEO), where both genes ranked among the most consistently dysregulated in rheumatoid arthritis, systemic lupus erythematosus, osteoarthritis, juvenile idiopathic arthritis. Data was retrieved mainly from Ensembl, and in some cases from UniProt, COSMIC, and NCBI databases.

To ensure biologically relevant variant evaluation, MANE Select and APPRIS principal transcripts were selected. For FAS, transcript ENST00000652046.1 (FAS-221) encoding a 335-amino-acid protein was used (UniProt: P25445-1; RefSeq: NM_000043.6) while for FASLG, transcript ENST00000367721.3 (FASLG-202) encoding a 281-amino-acid protein was selected (UniProt: P48023-1; RefSeq: NM_000639.3).

All SNVs for both genes were extracted from Ensembl. Only missense variants were selected for detailed analysis because of their direct impact on protein structure and function. Frameshift, nonsense, and splice-site variants validated in ClinVar were documented for reference but excluded from predictive modeling.

Missense variants were evaluated using a consensus approach with 12 independent *in-silico* tools, i.e., SIFT, PolyPhen-2, CADD, REVEL, MetaLR, MutationAssessor, Align-GVGD, PROVEAN, PANTHER, PhD-SNP, SNP&GO, and P-Mut, as described earlier. Variants predicted to be deleterious by the majority of tools were classified as high-confidence pathogenic candidates. Protein stability changes induced by missense mutations were predicted using MUpro and I-Mutant 2.0, which estimate direction and magnitude of free-energy changes (ΔΔG). Variants associated with significant destabilization were prioritized.Functional consequences of amino acid substitutions were assessed using MutPred2 while evolutionary conservation was evaluated using ConSurf. Conserved domain mapping was performed using PROSITE. NCBI Conserved Domain Database was used to determine whether mutations affected ligand-binding region, death domains, or TNF domains.

Three-dimensional models of wild-type and mutant FAS proteins were generated using SWISS-MODEL and validated using PROCHECK (Ramachandran plot analysis). Structural visualization was performed using UCSF Chimera. Protein–protein interactions were explored using GeneMANIA, while protein–ligand interactions were predicted using the COACH server.

Results

Mutational Spectrum and Pathogenic Variant Prioritization

A total of 11,386 variants were identified in FAS, including 392 missense, 35 frameshift, 31 splice acceptor, 37 splice donor, 149 synonymous, 16 stop-gained, and 2 stop-lost variants, along with a large number of low-impact variants (Figure 1). In FASLG, 258 missense variants were identified. In both cases, only missense variants were selected for downstream analysis because of their potential impact on protein structure and function.

Mutational Spectrum and Pathogenic Variant Prioritization

A total of 11,386 variants were identified in FAS, including 392 missense, 35 frameshift, 31 splice acceptor, 37 splice donor, 149 synonymous, 16 stop-gained, and 2 stop-lost variants, along with a large number of low-impact variants (Figure 1). In FASLG, 258 missense variants were identified. In both cases,

only missense variants were selected for downstream analysis because of their potential impact on protein structure and function. All 392 missense variants were evaluated using 12 in silico prediction tools to assess pathogenicity. SIFT classified 205 variants as deleterious, while REVEL identified 86 variants as likely disease-causing. PROVEAN predicted 135 variants to be functionally damaging, and MetaLR assigned high deleterious scores to 297 variants. The percentage distribution of FAS and FASLG variants by different *in silico* tools is summarized as Figure 2.

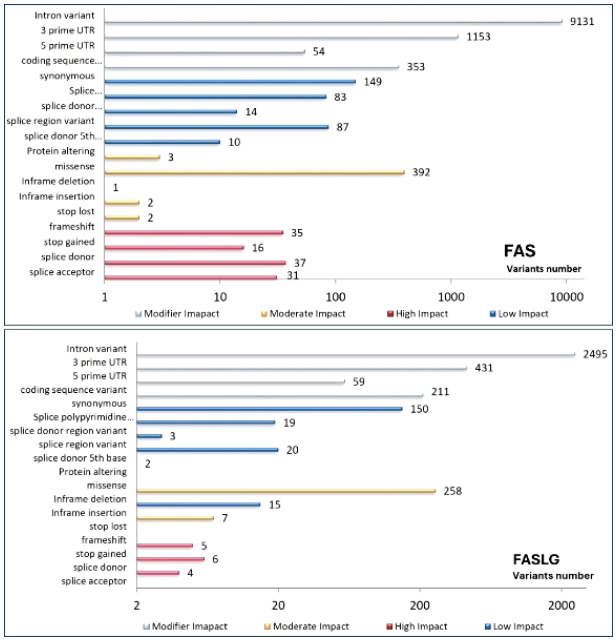

Figure 1. Total number and type of FAS-221 and FASLG variants, reported in Ensemble.

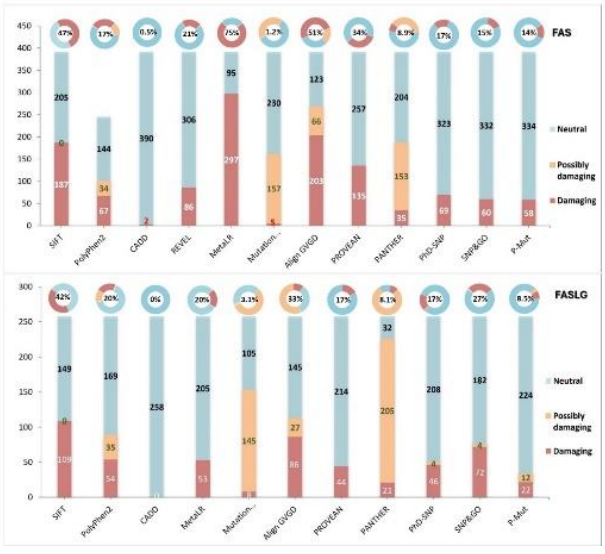

Figure 2. Distribution and percentage pathogenicity of FAS and FASLG variants across different computational tools.

Later, using consensus pathogenicity prediction, 82 high-confidence pathogenic variants were prioritized detailed analysis in FAS and 44 in FASLG (Figure. 2; Table I and II). The FAS G112S variant emerged as the most deleterious, being consistently classified as damaging across all tools. Several cysteine substitutions, including C101Y, C119Y/S, and C127G, were also predicted as highly damaging, indicating a high likelihood of functional disruption. For FASLG, G246R (rs867923082), G187R (rs1456004776), F276S (rs974185747), and W162R (rs2101810526) showed the strongest pathogenic signatures.

Stability, Conservation, and Domain Disruption

While combining the data of 82 consensus-selected deleterious variants of Ensemble and 62 ClinVar pathogenic variants (including 28 frameshift, 9 stop-gained, 13 splice donor, 6 splice acceptor, and 2 protein-altering variants, a mutational landscape mapping key mutation to their corresponding protein domain and exon location, was generated. This visualization revealed key mutation hotspots across cysteine-rich domains (CRD1–CRD3), the transmembrane (TM) region, and the death domain of FAS (Figure 3). This detailed mapping highlights how variations may structurally and functionally disrupt FAS-mediated apoptotic signaling. Further, protein stability analyses demonstrated that most prioritized variants in both FAS and FASLG significantly decreased protein stability (Supplementary Table S1, S2). Using MutPred2, 30 FAS variants with high pathogenic scores (>0.45) were identified out of 82.

ConSurf also revealed that many substitutions occurred at highly conserved residues. Conserved domain analysis showed clustering of 19 FAS variants within the “extracellular ligand-binding domain” (cd10579; residues 39–167) while the remaining were located within “intracellular death domain” (cd08316; residues 226–319); residue C59 was identified within the highly conserved CRD1 region (Figure. 4; top panel).

In case of FASLG, integration of MutPred2 and stability results lead to the shortlisting of 32 variants (mapped to 29 positions) for conservation analysis. Amongst these, 15 residues (P10, W162, L181, G187, R198, G202, H209, V211, G246, A247, N260, V267, T274, F276, G277) showed the highest conservation score of 9. Conserved domain analysis showed that 24 of the 29 conserved variants were located in the polypeptide-binding domain (cd00184; residues 146–279). PROSITE further confirmed that residues 145–281 belong to the highly conserved TNF homology domain (THD-2; PS50049). Mutations within this region are therefore expected to significantly affect ligand binding and signaling.

Structural and Interaction Analysis

DOI: 10.53389/RJAHS.2025040203

Table I: List of 82 missense variants of FAS along with corresponding score of *in-silico* pathogenicity prediction tool. (Red represents pathogenic/damaging; Yellow: likely pathogenic/uncertain significance;

Sr. No	Variant ID	Alleles	ClinVar Status	Amino Acid Change	SIFT	PolyPhen	CADD	REVEL	MetaLR	Mutation Assessor	AlignGVGD	PROVEAN	PANTHER	PhD-SNP	SNPs&GO	PMut
1	rs2133503818	G/A		C101Y	0	1	26	0.889	0.996	0.952	193.72 (C65)	-9.105	0.57	0.836	0.917	0.89 (92%)
2	rs2133513826	G/A/C		C119Y	0	1	24	0.718	0.996	0.952	193.72 (C65)	-9.044	0.57	0.869	0.898	0.90 (93%)
3	rs2133513826	G/A/C		C119S	0	1	24	0.704	0.996	0.952	111.67 (C65)	-8.183	0.57	0.814	0.864	0.89(92%)
4	rs1848386782	T/G	?	C127G	0	1	27	0.949	0.996	0.952	158.23 (C65)	-9.858	0.57	0.759	0.898	0.90 (93%)
5	rs2133504146	G/A		G112S	0	0.999	32	0.806	0.9	0.935	55.27 (C55)	-4.025	0.57	0.664	0.698	0.82 (90%)
6	rs2133502994	G/A		C85Y	0	0.595	25	0.646	0.995	0.925	193.72 (C65)	-8.225	0.57	0.755	0.771	0.83 (90%)
7	rs2133503019	C/G/T		C85W	0	0.993	22	0.713	0.995	0.925	214.36 (C65)	-8.212	0.57	0.726	0.752	0.90 (93%)
8	rs1036815834	G/A		G88R	0.03	0.999	25	0.783	0.835	0.917	125.13 (C65)	-5.525	0.57	0.592	0.461	0.40 (86%)
9	rs1480416112	C/T		T120I	0	1	19	0.316	0.818	0.893	89.28 (C65)	-4.713	0.5	0.548	0.406	0.46 (84%)
10	rs2133503469	G/C		D93H	0	0.998	24	0.568	0.86	0.889	81.24 (C65)	-4.426	0.5	0.405	0.523	0.34 (88%)
11	rs2133514173	G/T		K126N	0	0.976	23	0.561	0.821	0.865	93.88 C65)	-3.038	0.5	0.406	0.301	0.43 (85%)
12	rs749714005	A/C/G	?	E116G	0	0.997	25	0.644	0.814	0.861	97.85 (C65)	-4.614	0.5	0.479	0.41	0.47 (84%)
13	rs121913080	G/A/C	⚠⚠	R250Q	0		26	0.89	0.943	0.859	42.81 (C35)	-2.962	0.57	0.753	0.62	0.78 (88%)
14	rs121913080	G/A/C	⚠⚠	R250P	0		26	0.948	0.932	0.859	102.71 (C65)	-5.583	0.57	0.843	0.784	0.84 (90%)
15	rs1589491089	A/C/G	?⚠	E272A	0		24	0.836	0.914	0.859	106.71 (C65)	-4.95	0.5	0.548	0.299	0.81 (89%)
16	rs1589491089	A/C/G	?⚠	E272G	0		25	0.909	0.914	0.859	97.85 (C65)	-5.556	0.5	0.488	0.293	0.81 (89%)
17	rs2119446879	G/A	?	G286E	0.01		25	0.785	0.885	0.859	97.85 (C65)	-6.219	0.57	0.843	0.735	0.71 (86%)
18	rs2119447036	G/A		A290T	0		23	0.364	0.663	0.859	58.02 (C55)	-3.115	0.5	0.615	0.429	0.74 (87%)
19	rs760993872	C/A/T	?	A290E	0		23	0.829	0.772	0.859	106.71 (C65)	-3.893	0.5	0.738	0.525	0.72 (86%)
20	rs760993872	C/A/T	?	A290V	0		23	0.453	0.772	0.859	64.43 (C55)	-3.115	0.5	0.556	0.387	0.76 (88%)
21	rs1848315820	A/G	⚠	D108G	0	1	28	0.821	0.801	0.851	93.77 (C65)	-5.159	0.57	0.691	0.761	0.79 (89%)
22	rs2119445351	A/G	?	M240V	0		23	0.635	0.833	0.851	21.52 (C35)	-3.017	0.5	0.761	0.551	0.64 (84%)
23	rs2119445378	T/A	?	M240K	0		23	0.781	0.898	0.851	94.49 (C65)	-4.575	0.5	0.878	0.772	0.65 (84%)
24	rs121913086	G/A/T	⚠⚠	D260N	0		28	0.762	0.903	0.851	23.01 (C35)	-3.732	0.5	0.475	0.504	0.49 (83%)
25	rs121913086	G/A/T	⚠⚠	D260Y	0		27	0.895	0.904	0.851	159.94 (C65)	-6.758	0.5	0.655	0.669	0.54 (80%)
26	rs28929498	A/T	⚠	D260V	0		27	0.898	0.898	0.851	152.01 (C65)	-6.769	0.5	0.56	0.637	0.66 (85%)
27	rs1848675068	T/C	?	I259T	0		26	0.875	0.937	0.849	89.28 (C65)	-3.921	0.5	0.746	0.725	0.69 (86%)
28	rs200778245	T/C/G	?	V245G	0		23	0.593	0.675	0.844	108.79 (C65)	-5.047	0.5	0.748	0.841	0.67 (85%)
29	rs2119445876	G/A		E256K	0		28	0.601	0.874	0.844	56.87 (C55)	-2.837	0.5	0.682	0.554	0.68 (85%)
30	rs483352683	T/A/C	?⚠	I262N	0		25	0.793	0.918	0.839	148.91 (C65)	-3.95	0.5	0.689	0.483	0.55 (80%)
31	rs2119446558	A/C	?	Q276P	0		24	0.726	0.886	0.839	75.14 (C65)	-3.783	0.5	0.696	0.619	0.56 (81%)
32	rs121913081	C/T	?⚠	T270I	0		22	0.596	0.772	0.833	89.28 (C65)	-4.114	0.5	0.372	0.114	0.44 (85%)
33	rs770556399	A/G		H285R	0		24	0.575	0.741	0.833	28.82 (C35)	-5.063	0.5	0.594	0.409	0.40 (86%)
34	rs1274696891	G/A		A307T	0		22	0.436	0.799	0.831	58.02 (C55)	-2.645	0.57	0.47	0.257	0.53 (80%)
35	rs1848671126	G/T	⚠	G253V	0		23	0.433	0.763	0.829	108.79 (C65)	-5.367	0.5	0.524	0.466	0.66 (85%)
36	rs2119448150	T/G	?	I310S	0		23	0.682	0.895	0.821	141.8 (C65)	-3.572	0.5	0.763	0.643	0.51 (79%)
37	rs1848312375	A/C		E87A	0	0.993	25	0.6	0.818	0.819	106.71 (C65)	-3.744	0.5	0.304	0.157	0.26 (90%)
38	rs544766724	A/C		K251T	0		23	0.552	0.755	0.816	77.74 (C65)	-3.576	0.5	0.331	0.308	0.42 (85%)
39	rs2119446013	A/T		E261V	0		25	0.679	0.898	0.813	121.33 (C65)	-4.967	0.5	0.309	0.105	0.34 (88%)
40	rs121913078	C/T	⚠	R121W	0.02	0.983	22	0.539	0.834	0.798	101.29 (C65)	-3.574	0.19	0.332	0.349	0.14 (94%)
41	rs2133503428	C/T		T92I	0	0.947	22	0.674	0.804	0.797	89.28 (C65)	-1.957	0.5	0.222	0.159	0.14 (94%)
42	rs1365404574	T/A		S230R	0.04		21	0.42	0.848	0.781	109.21 (C65)	-3.035	0.5	0.631	0.394	0.29 (89%)
43	rs781035943	T/A		V275D	0		25	0.803	0.859	0.779	152.01 (C65)	-4.531	0.5	0.711	0.668	0.46 (84%)
44	rs1404280764	G/C/T	?	C135S	0	1	25	0.6	0.783	0.75	111.67 (C65)	-8.261	0.57	0.796	0.9	0.85 (91%)
45	rs1404280764	G/C/T	?	C135F	0	1	26	0.613	0.783	0.75	204.39 (C65)	-9.091	0.57	0.832	0.911	0.85 (91%)
46	rs1161840202	T/G		C140G	0	1	26	0.712	0.815	0.75	158.23 (C65)	-9.235	0.57	0.832	0.929	0.78 (88%)
47	rs1848390240	G/A		C140Y	0	1	24	0.71	0.822	0.75	193.72 (C65)	-8.71	0.57	0.857	0.924	0.79 (89%)
48	rs1848473290	T/C		C149R	0	1	25	0.899	0.996	0.75	179.53 (C65)	-9.23	0.57	0.779	0.919	0.90 (93%)
49	rs2133527321	G/A		C157Y	0	1	23	0.798	0.996	0.75	193.72 (C65)	-8.858	0.57	0.772	0.867	0.78 (88%)
50	rs2133527819	T/A		C165S	0	1	23	0.797	0.996	0.75	111.67 (C65)	-7.929	0.57	0.598	0.714	0.89 (92%)
51	rs1442207718	A/G		T125A	0.04	0.987	23	0.773	0.881	0.745	58.02 (C55)	-2.84	0.5	0.157	0.1	0.25 (91%)
52	rs483352683	T/A/C	?⚠	I262T	0		24	0.865	0.902	0.745	89.28 (C65)	-2.538	0.5	0.379	0.272	0.12 (95%)
53	rs1589482007	G/C		G152R	0	0.999	24	0.741	0.899	0.742	125.13 (C65)	-5.967	0.57	0.481	0.567	0.74 (87%)
54	rs121913079	A/G	?⚠	Y232C	0		24	0.718	0.862	0.729	193.72 (C65)	-6.398	0.5	0.713	0.677	0.37 (87%)
55	rs1462888256	C/A		T160N	0	0.997	20	0.368	0.851	0.726	64.77 (C55)	-3.868	0.02	0.531	0.488	0.58 (82%)
56	rs749714005	A/C/G	?	E116A	0	0.995	24	0.533	0.807	0.715	106.71 (C65)	-3.499	0.5	0.463	0.328	0.09 (96%)
57	rs2119446323	C/A/T		A271E	0		22	0.514	0.685	0.712	106.71 (C65)	-2.699	0.5	0.436	0.328	0.34 (88%)
58	rs984333050	C/A		H142Q	0	0.993	22	0.452	0.818	0.709	106.71 (C65)	-4.961	0.5	0.603	0.796	0.44 (85%)
59	rs1281548561	C/T		T158I	0	0.988	22	0.667	0.852	0.707	89.28 (C65)	-4.729	0.5	0.397	0.521	0.84 (90%)
60	rs1366487814	A/T		N132I	0	0.998	25	0.602	0.552	0.692	148.91 (C65)	-6.407	0.5	0.487	0.612	0.74 (87%)
61	rs1848473930	A/G/T		H151L	0	0.994	24	0.52	0.771	0.688	98.69 (C65)	-6.216	0.5	0.393	0.287	0.38 (87%)
62	rs200864612	A/G	?	D317G	0		22	0.517	0.866	0.685	93.77 (C65)	-2.886	0.5	0.41	0.213	0.37 (87%)
63	rs993150748	A/G/T	?	N162I	0	0.99	22	0.503	0.863	0.668	148.91 (C65)	-5.905	0.19	0.281	0.284	0.62 (83%)
64	rs773565107	G/A		E114K	0	0.995	26	0.695	0.82	0.638	56.87 (C55)	-2.768	0.5	0.665	0.721	0.33 (88%)
65	rs563551720	C/A/G/T	?	T163N	0	0.972	18	0.371	0.91	0.638	64.77 (C55)	-3.764	0.5	0.427	0.4	0.56 (81%)
66	rs563551720	C/A/G/	?	T163I	0	0.962	19	0.432	0.908	0.638	89.28 (C65)	-4.414	0.5	0.318	0.343	0.59 (82%)
67	rs764567970	T/C	?	L242P	0		22	0.567	0.616	0.581	97.78 (C65)	-4.374	0.19	0.826	0.648	0.51 (79%)
68	rs2133470780	C/A/T		A25D	0	0.962	17	0.511	0.809	0.577	125.75 (C65)	-2.245	0.5	0.584	0.482	0.19 (93%)
69	rs886047459	G/A/T	?	C59Y	0	0.999	23	0.596	0.569	0.577	193.72 (C65)	-7.722	0.57	0.821	0.926	0.75 (87%)
70	rs886047459	G/A/T	?	C59F	0	0.999	23	0.597	0.569	0.577	204.39 (C65)	-7.822	0.57	0.736	0.889	0.85 (91%)
71	rs2133472256	G/A		C63Y	0	0.999	23	0.742	0.948	0.577	193.72 (C65)	-8.722	0.57	0.797	0.911	0.88 (92%)
72	rs1345570456	C/T		P65S	0	0.931	17	0.376	0.596	0.577	73.35 (C65)	-3.308	0.5	0.275	0.324	0.17 (93%)
73	rs751654768	T/C/G	?	C73R	0	0.999	24	0.552	0.568	0.577	179.53 (C65)	-8.493	0.57	0.749	0.907	0.90 (93%)
74	rs751654768	T/C/G	?	C73G	0	0.999	24	0.486	0.568	0.577	158.23 (C65)	-8.493	0.57	0.731	0.922	0.89 (92%)
75	rs2133502355	G/A/C	?	C73Y	0.04	0.999	24	0.412	0.552	0.577	193.72 (C65)	-7.955	0.57	0.771	0.881	0.90 (93%)
76	rs2133502355	G/A/C	?	C73S	0	0.999	23	0.495	0.552	0.577	111.67 (C65)	-7.239	0.57	0.742	0.884	0.90 (93%)
77	rs1848490280	T/A/G	?	L177R	0.03	0.987	22	0.311	0.855	0.574	101.88 (C65)	-2.763	0.5	0.569	0.498	0.32 (89%)
78	rs121913083	A/G	⚠	N118S	0.04	0.961	21	0.34	0.801	0.57	46.24 (C35)	-3.326	0.5	0.432	0.55	0.46 (84%)
79	rs775652162	T/G		F134V	0	0.979	25	0.6	0.862	0.564	49.94 (C35)	-4.775	0.19	0.531	0.601	0.75 (87%)
80	rs1848491248	T/C		L180P	0	0.975	18	0.355	0.857	0.564	97.78 (C65)	-2.4	0.19	0.842	0.736	0.44 (85%)
81	rs1435894576	A/T		E114V	0	0.998	32	0.699	0.749	0.445	121.33 (C65)	-5.091	0.5	0.627	0.721	0.37 (87%)
82	rs1353528671	T/C		L10P	0.04	0.046	22	0.617	0.768	0.403	97.78 (C65)	-2.742	0.5	0.779	0.719	0.46 (84%)

PROSITE analysis identified six disulfide bonds within the extracellular domain of FAS. High-risk cysteine substitutions directly disrupted several of these bonds. In FASLG, three high-confidence N-linked glycosylation sites were identified at N184, N250, and N260. Variants such as N184K, N250D, and N260K were predicted to abolish these glycosylation sites, potentially impairing ligand folding and receptor binding. Structural modeling of three high-risk FAS variants—C85Y, C119Y, and

C127G—revealed complete loss of disulfide bonds and marked distortion of the extracellular domain (Figure 5). These results confirm a severe destabilization of the extracellular domain due to cysteine substitutions.

Further, protein–protein interaction analysis confirmed tight functional coupling of FAS with FADD, CASP8, CASP10, **protein kinase III respectively, that act as modulators in death receptors**.

TRADD, CFLAR, and FASLG (Figure 6). Protein–ligand interaction analysis predicted Zn^{2+} as a key ligand for FAS and peptide ligands for FASLG, with several pathogenic variants located at predicted binding sites.

Table II: List of 44 missense variants of FASLG along with corresponding score of *in-silico* pathogenicity prediction tool. (Red represents pathogenic/damaging; Yellow: likely pathogenic/uncertain significance; Green: benign)

Sr. No.	Variant ID	Alleles	ClinVar Status	Amino Acid Change	SIFT	PolyPhen	CADD	MetaLR	Mutation Assessor	Align GVGD	PROVEAN	PANTHER	PhD-SNP	SNP&GO	P-Mut
1	rs2101810526	T/C	?	W162R	0	1	28	0.949	0.937	101.29 (C65)	-12.357	0.85	0.72	0.859	0.90 (93%)
2	rs1456004776	G/A		G187R	0	1	28	0.997	0.936	125.13 (C65)	-7.638	0.85	0.931	0.93	0.90 (93%)
3	rs12079514	A/C		Y189S	0	1	27	0.981	0.936	143.11 (C65)	-8.67	0.85	0.941	0.953	0.87 (92%)
4	rs974185747	T/C		F276S	0	0.999	28	0.673	0.936	154.81 (C65)	-7.56	0.85	0.726	0.877	0.90 (93%)
5	rs1413244355	G/A	?	G277S	0	1	29	0.886	0.936	55.27 (C35)	-5.67	0.85	0.423	0.731	0.84 (90%)
6	rs867923082	G/A/C		G246R	0	0.998	29	0.584	0.934	125.13 (C65)	-7.704	0.85	0.817	0.901	0.90(93%)
7	rs867923082	G/A/C		G246R	0	0.998	29	0.584	0.934	125.13 (C65)	-7.704	0.85	0.817	0.901	0.90(93%)
8	rs1659251393	G/A		G246E	0	0.998	28	0.584	0.934	97.85 (C65)	-7.704	0.85	0.817	0.92	0.88 (92%)
9	rs2101810634	G/C	?	C202S	0	0.999	26	0.887	0.929	111.67 (C65)	-5.373	0.57	0.755	0.862	0.76 (88%)
10	rs773263762	C/T		L181F	0	1	24	0.963	0.921	21.82 (C15)	-3.708	0.57	0.665	0.668	0.71 (86%)
11	rs1205013237	C/T	?	R198W	0	0.994	26	0.91	0.905	101.29 (C65)	-4.886	0.74	0.796	0.842	0.88 (92%)
12	rs80358237	C/A	?	A247E	0	0.986	24	0.352	0.899	106.71 (C65)	-3.527	0.5	0.788	0.855	0.86(91%)
13	rs747293631	T/G		V182G	0	0.832	25	0.889	0.893	108.79 (C65)	-4.898	0.5	0.773	0.811	0.71 (86%)
14	rs1473699993	G/A/T	?	V211F	0	0.966	25	0.468	0.891	49.94 (C45)	-3.302	0.5	0.561	0.573	0.80 (89%)
15	rs1659253812	C/A		T274K	0	0.991	26	0.573	0.891	77.74 (C65)	-3.643	0.57	0.512	0.651	0.89 (92%)
16	rs1280905898	C/T		H209Y	0	0.999	26	0.902	0.883	83.33 (C65)	-4.444	0.57	0.595	0.593	0.79 (89%)
17	rs1347125362	A/G		Y176C	0	1	27	0.895	0.881	193.72 (C65)	-7.615	0.5	0.704	0.82	0.87 (91%)
18	rs1455255180	G/C/T		V267F	0	0.88	24	0.864	0.876	49.94 (C45)	-3.667	0.5	0.669	0.585	0.65 (84%)
19	rs1396406162	T/C		F276L	0	0.999	20	0.586	0.866	21.82 (C15)	-5.67	0.85	0.606	0.814	0.56 (81%)
20	rs1188616579	C/T		S265F	0	0.834	25	0.825	0.853	154.81 (C65)	-3.202	0.5	0.425	0.552	0.47 (83%)
21	rs1385875080	G/A/C/T		G199D	0.05	0.968	22	0.878	0.828	93.77 (C65)	-4.294	0.5	0.797	0.843	0.34 (88%)
22	rs1263388490	A/G		Y212C	0.02	0.98	23	0.815	0.809	193.72 (C65)	-5.2	0.5	0.403	0.662	0.52 (79%)
23	rs1181894131	T/C		L278S	0	1	26	0.331	0.802	144.08 (C65)	-1.483	0.5	0.141	0.377	0.71 (86%)
24	rs559770662	C/G		P219R	0.01	0.701	20	0.674	0.798	102.71 (C65)	-5.956	0.74	0.576	0.744	0.26 (91%)
25	rs1310181064	A/G		Y196C	0	0.655	24	0.741	0.795	193.72 (C65)	-2.379	0.5	0.586	0.775	0.41(86%)
26	rs780397117	C/T		P10S	0	0.998	25	0.185	0.788	73.35 (C65)	-2.481	0.57	0.675	0.615	0.66 (84%)
27	rs1659092349	G/C		G98A	0.04	0.998	24	0.156	0.788	60.00 (C55)	-1.256	0.5	0.601	0.743	0.47 (83%)
28	rs886045569	G/A/C	?	W14C	0.01	0.957	27	0.185	0.781	214.36 (C65)	-3.086	0.5	0.866	0.726	0.59 (82%)
29	rs1162126723	A/G		D16G	0	0.997	25	0.119	0.775	93.77 (C65)	-2.097	0.5	0.72	0.606	0.40 (86%)
30	rs376317481	A/G/T	?	N250I	0.01	0.96	23	0.799	0.773	148.91 (C65)	-3.065	0.5	0.384	0.716	0.42 (85%)
31	rs771262843	T/C/G	+	N184K	0	0.98	21	0.821	0.75	93.88 (C65)	-1.956	0.5	0.486	0.711	0.49 (83%)
32	rs753445258	C/T		T252I	0.02	0.918	24	0.814	0.75	89.28 (C65)	-2.748	0.5	0.552	0.716	0.36 (87%)
33	rs780519407	A/G		Y279C	0	0.993	25	0.837	0.749	193.72 (C65)	-5.712	0.5	0.14	0.461	0.40 (86%)
34	rs2101806668	G/A		G96R	0	0.36	28	0.076	0.74	125.13 (C65)	-3.501	0.5	0.751	0.811	0.55 (81%)
35	rs771815134	A/T		Q237L	0.01	0.136	21	0.642	0.74	112.44 (C65)	-3.896	0.5	0.472	0.695	0.40 (86%)
36	rs1659244824	T/C		I183T	0	0.924	25	0.435	0.733	89.28 (C65)	-3.462	0.5	0.844	0.87	0.57 (82%)
37	rs778993712	C/A		S172Y	0	0.997	25	0.318	0.707	143.11 (C65)	-2.697	0.5	0.455	0.767	0.42 (85%)
38	rs760032192	C/A/G	?	L188V	0.03	0.198	16	0.737	0.706	31.78 (C25)	-1.056	0.57	0.647	0.619	0.22 (92%)
39	rs763787856	C/T		R241C	0	0.822	28	0.72	0.661	179.53 (C65)	-3.128	0.13	0.67	0.784	0.37 (87%)
40	rs1385875080	G/A/C/T		G199A	0.01	0.567	23	0.792	0.654	60.00 (C55)	-3.372	0.5	0.589	0.655	0.44 (85%)
41	rs1571333759	T/C	?	V248A	0.01	0.294	23	0.698	0.606	64.43 (C55)	-2.952	0.5	0.483	0.567	0.53 (80%)
42	rs1385875080	G/A/C/T		G199V	0	0.968	24	0.88	0.581	108.79 (C65)	-5.059	0.5	0.772	0.855	0.39 (82%)
43	rs776079129	T/C		F197L	0.01	0.535	21	0.796	0.577	21.82 (C15)	-3.062	0.74	0.628	0.624	0.76 (88%)
44	rs761374744	C/A/T	+	N260K	0.01	0.994	14	0.796	0.555	93.88 (C65)	-2.782	0.57	0.584	0.661	0.67 (85%)

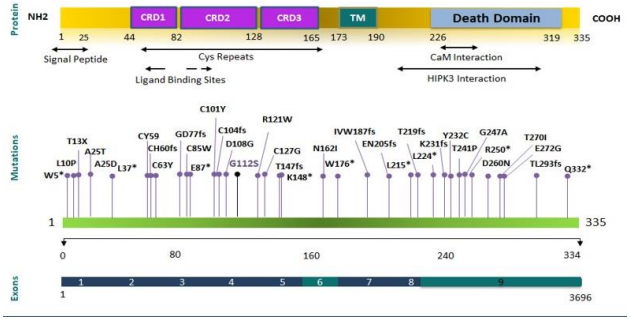

Figure 3. Mutational architecture of FAS gene. CRD1, CRD2 and CRD3 represent cysteine rich domains, these are conserved structural motifs of the extracellular ligand binding sites. TM is transmembrane domain. CaM and HIPK3 are calmodulin and homeodomain interacting

Discussion

Disruption of programmed cell death pathway has long been recognized as a central driver of immune dysregulation and cancer development.[16,17] *The clinical importance of this pathway is best illustrated by autoimmune lymphoproliferative* syndrome (ALPS), a disorder caused primarily by heterozygous mutations in FAS that impair apoptotic deletion of lymphocytes.[7,18] Beyond ALPS, polymorphisms in FAS and FASLG have been associated with a wide spectrum of autoimmune conditions, including systemic lupus erythematosus, multiple sclerosis, rheumatoid arthritis, autoimmune thyroid disease, as well as with hematological and solid malignancies.[7,18-22]

DOI: 10.53389/RJAHS.2025040203

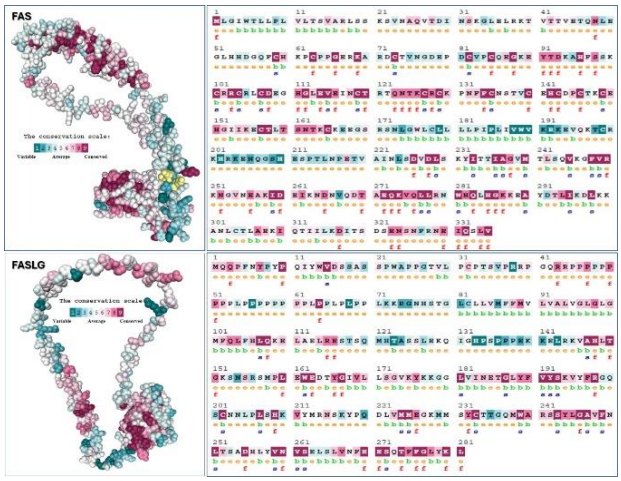

Figure 4. Consurf analysis of FAS-221 and FASLG. Models are colored by conservation score of each residue.

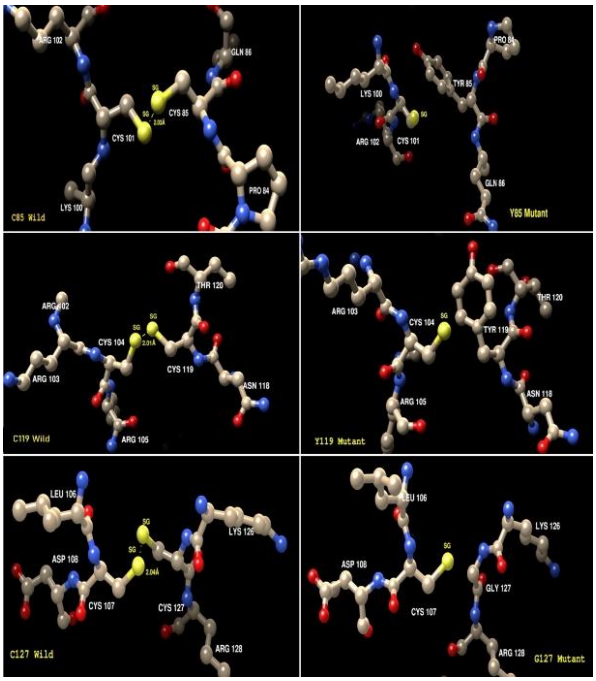

Figure 5. Structure analysis of FAS variants by UCSF chimera. The wild type C85 protein (top left) shows disulfide bond with C101; C119 (wild type-middle left) shows disulfide bond with C104; C127 (wild type-lower left) shows disulfide bond with C107. Loss of disulfide bonds and corresponding changes in interactions are evident.

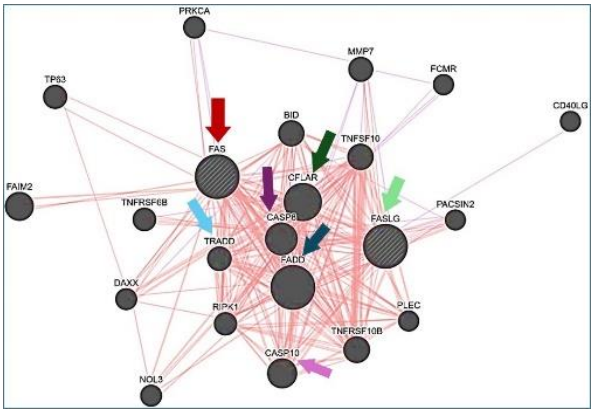

Figure 6. Protein-protein interaction analyses through GeneMania. Besides FASLG (marked with green arrow), FADD, CASP8/10, CFLAR, TNFSF10, and TRADD are close interacting partners of FAS (marked with red arrow).

Despite the clear clinical relevance of the Fas/FasL system, a systematic in silico dissection of FAS/FASLG variants has been limited. Since advances in computational biology now allow reliable prediction of the pathogenicity of different variants.[14,23-26], we, in the present work, applied a comprehensive consensus of advanced pathogenicity prediction tools to analyze 392 missense variants in FAS and 258 in FASLG. This integrative approach allowed us to minimize algorithm-specific bias and to prioritize variants most likely to exert true biological effects. [15]

Among the FAS variants, G112S emerged as the most consistently deleterious substitution across all prediction platforms. In addition, several cysteine substitutions—including C101Y, C119Y/S, and C127G—were found to carry a high likelihood of pathogenicity. For FASLG, G246R, G187R, F276S, and W162R that are located within highly conserved regions, showed the strongest deleterious signatures. The convergence of pathogenicity and stability predictions in our dataset further revealed that many of the prioritized variants in FAS/FASLG, especially those involving substitution of 'evolutionary conserved cysteine' residues, may have strong impact on structural stability, ligand binding or receptor activation.

Protein destabilization is a well-established mechanism and disulfide bonds play a fundamental role in stabilizing the tertiary structure of extracellular proteins; mutations that lead to improper protein folding, loss of function, and aberrant degradation are frequently implicated in both inherited disorders and cancers.[27] In this study, functional prediction using MutPred2 showed that some of the prioritized pathogenic FAS variants are likely to disrupt disulfide bond formation within the extracellular ligand-binding domain and the intracellular death domain—two regions essential for apoptotic signaling. Likewise, in FASLG, several high-risk variants (particularly at N184, N250, and N260) were found within the highly conserved TNF

homology domain, which governs ligand trimerization and receptor interaction.[5,12,28,29], highlighting multiple structural routes through which FASLG function may be impaired. Protein–ligand interaction analysis added an additional layer of functional validation. Zinc was predicted as a key ligand interacting with FAS at cysteine-rich regions of the extracellular domain, further emphasizing the functional importance of C85, C119, and C127. To directly visualize the structural consequences of cysteine substitutions, three-dimensional structural modeling were performed. All mutant models demonstrated complete loss of their corresponding disulfide bonds and exhibited marked distortion of the extracellular domain when compared with the wild-type structure. These findings provide compelling structural evidence that loss of disulfide bond integrity is a major mechanism by which deleterious FAS mutations disrupt receptor function.

Taken together, the results of this study demonstrate that pathogenic missense variants in FAS and FASLG are not randomly distributed but instead are highly enriched within structurally and functionally critical domains. Substitutions that disrupt disulfide bonds, glycosylation sites, ligand-binding interfaces, and overall protein stability emerge as the most detrimental. These molecular disturbances offer a coherent explanation for how subtle amino acid changes can exert dominant-negative or loss-of-function effects on apoptotic signaling and drive immune dysregulation. Recent studies continue to reinforce the clinical relevance of these mechanisms. Large-scale sequencing efforts in patients with immune dysregulation syndromes have increasingly identified rare missense variants in apoptotic pathway genes, including FAS and FASLG, as key contributors to disease heterogeneity.[13,25] Moreover, defects in Fas-mediated apoptosis are now being explored as potential biomarkers for immune checkpoint therapy resistance and for stratifying patients with lymphoproliferative disorders.[28,29,30]

Nevertheless, despite the strength of computational predictions, in silico findings cannot substitute for experimental validation.[24,31] Functional assays in cellular systems and in vivo models will be necessary to confirm the predicted effects on receptor signaling, DISC formation, caspase activation, and lymphocyte survival. Such studies will be essential to establish definitive genotype–phenotype relationships and to translate these findings into clinical practice.

Conclusions

This work delineates key pathogenic variants within the FAS/FASLG axis, provides mechanistic insights into how disrupted apoptosis contributes to immune dysregulation, and sets a foundation for their future experimental validation.

References

1. Chowdhury I, Tharakan B, Bhat GK. Current concepts in apoptosis: the physiological suicide program revisited. Cell Mol Biol Lett. 2006;11:506–525. https://doi.org/10.2478/s11658-006-0041-3
2. Kiraz Y, Adan A, Kartal Yandim M, Baran Y. Major apoptotic mechanisms and genes involved in apoptosis. Tumour Biol. 2016;37:8471–8486. https://doi.org/10.1007/s13277-016-5035-9
3. Koshkina N, Yang Y, Kleinerman ES. The Fas/FasL signaling pathway: its role in the metastatic process and as a target for treating osteosarcoma lung metastases. In: Current Advances in the Science of Osteosarcoma. 2020. p. 177–187. https://doi.org/10.1007/978-3-030-43085-6_12
4. Aggarwal BB, Singh S, LaPushin R, Totpal K. Fas antigen signals proliferation of normal human diploid fibroblast and its mechanism is different from tumor necrosis factor receptor. FEBS Lett. 1995;364(1):5–8. https://doi.org/10.1016/0014-5793(95)00339-B
5. Arakaki R, Yamada A, Kudo Y, Hayashi Y, Ishimaru N. Mechanism of activation-induced cell death of T cells and regulation of FasL expression. Crit Rev Immunol. 2014;34(4). https://doi.org/10.1615/CritRevImmunol.2014009988
6. Janda A, Schwarz K, van der Burg M, Vach W, Ijspeert H, Lorenz MR, et al. Disturbed B-lymphocyte selection in autoimmune lymphoproliferative syndrome. Blood. 2016;127(18):2193–2202. https://doi.org/10.1182/blood-2015-04-642488
7. Magerus-Chatinet A, Neven B, Stolzenberg MC, Daussy C, Arkwright PD, Lanzarotti N, et al. Onset of autoimmune lymphoproliferative syndrome in humans as a consequence of genetic defect accumulation. J Clin Invest. 2011;121(1):106–112. https://doi.org/10.1172/JCI43752
8. Agrebi N, Ben-Mansour LS, Medhaffar M, Hadiji S, Fedhila F, Ben-Ali M, et al. Autoimmune lymphoproliferative syndrome caused by homozygous FAS mutations with normal or residual protein expression. J Allergy Clin Immunol. 2017;140(1):298–301.e293. https://doi.org/10.1016/j.jaci.2016.11.033
9. Kimura M, Matsuzawa A. Autoimmunity in mice bearing lprcs: a novel mutant gene. Int Rev Immunol. 1994;11(3):193–210. https://doi.org/10.3109/08830189409061727
10. Davidson WF, Giese T, Fredrickson TN. Spontaneous development of plasmacytoid tumors in mice with defective Fas-Fas ligand interactions. J Exp Med. 1998;187(11):1825–1838. https://doi.org/10.1084/jem.187.11.1825
11. Hughes MA, Harper N, Butterworth M, Cain K, Cohen GM, MacFarlane M. Reconstitution of the death-inducing signaling complex reveals a substrate switch that determines CD95-mediated death or survival. Mol Cell. 2009;35(3):265–279. https://doi.org/10.1016/j.molcel.2009.06.012
12. Guégan JP, Legembre P. Nonapoptotic functions of Fas/CD95 in the immune response. FEBS J. 2018;285(5):809–827. https://doi.org/10.1111/febs.14292
13. Karki R, Pandya D, Elston RC, Ferlini C. Defining mutation and polymorphism in the era of personal genomics. BMC Med Genomics.2015;8:37. https://doi.org/10.1186/s12920-015-0115-z
14. Li B, Krishnan VG, Mort ME, Xin F, Kamati KK, Cooper DN, et al. Automated inference of molecular mechanisms of disease from amino acid substitutions. Bioinformatics. 2009;25(21):2744–2750. https://doi.org/10.1093/bioinformatics/btp528
15. Tahir S, Rahim J, Sadaf S. In-silico prioritization of pathogenic interleukin-37b variants and a fusion platform for high-yield

soluble production. Biochimie. 2025;238(Pt B):102–111. https://doi.org/10.1016/j.biochi.2025.07.026
16. Aggarwal BB. Signalling pathways of the TNF superfamily: a double-edged sword. Nat Rev Immunol. 2003;3(9):745–756. https://doi.org/10.1038/nri1184
17. Croft M, Salek-Ardakani S, Ware CF. Targeting the TNF and TNFR superfamilies in autoimmune disease and cancer. Nat Rev Drug Discov. 2024:1–23. https://doi.org/10.1038/s41573-024-01053-9
18. De Bielke MGS, Yancoski J, Rocco C, Pérez LE, Cantisano C, Pérez N, et al. A missense mutation in the extracellular domain of Fas: founder effect in Argentinean ALPS patients. J Clin Immunol.2012;32(6):1197. https://doi.org/10.1007/s10875-012-9731-y
19. Li C, Larson D, Zhang Z, Liu Z, Strom SS, Gershenwald JE, et al. Polymorphisms of the FAS and FAS ligand genes associated with risk of cutaneous malignant melanoma. Pharmacogenet Genomics.2006;16(4):253–263. https://doi.org/10.1097/01.fpc.0000199501.54466.de
20. Erdogan M, Kulaksizoglu M, Ganidagli S, Berdeli A. Fas/FasL gene polymorphism in patients with Hashimoto's thyroiditis in Turkish population. J Endocrinol Invest. 2017;40:77–82. https://doi.org/10.1007/s40618-016-0534-5
21. Gormus U, Ergen A, Yaylim-Eraltan I, Yilmaz H, Turna A, Bozkurt N, Isbir T. Fas-1377 A/G polymorphism in lung cancer. In Vivo. 2007;21(4):663–666.
22. Farre L, Bittencourt A, Silva-Santos G, Almeida A, Silva A, Decanine D, et al. Fas–670 promoter polymorphism is associated with susceptibility, clinical presentation, and survival in adult T cell leukemia. J Leukoc Biol. 2008;83(1):220–222. https://doi.org/10.1189/jlb.0407198
23. Duarte AJ, Ribeiro D, Moreira L, Amaral O. In silico analysis of missense mutations as a first step in functional studies: examples from two sphingolipidoses. Int J Mol Sci. 2018;19(11):3409. https://doi.org/10.3390/ijms19113409
24. Garcia FAO, De Andrade ES, Palmero EI. Insights on variant analysis in silico tools for pathogenicity prediction. Front Genet. 2022;13:1010327. https://doi.org/10.3389/fgene.2022.1010327
25. Pasha U, Hanif K, Nisar H, et al. A novel missense compound heterozygous variant in TLR1 gene associated with susceptibility to rheumatoid arthritis. Clin Rheumatol. 2023;42:3097–3111. https://doi.org/10.1007/s10067-023-06702-9
26. Pasha U, Nisar H, Nisar H, Abid R, Ashraf NM, Sadaf S. Molecular dynamic simulations of missense mutation in PTPN22 and predisposition to rheumatoid arthritis. J Interferon Cytokine Res.2023;43(3):121–132. https://doi.org/10.1089/jir.2022.0216
27. Dobson CM. Protein folding and misfolding. Nature. 2003;426(6968):884–890. https://doi.org/10.1038/nature02261
28. Dowdell KC, Niemela JE, Price S, Davis J, Hornung RL, Oliveira JB, et al. Somatic FAS mutations in genetically undefined autoimmune lymphoproliferative syndrome. Blood. 2010;115(25):5164–5169. https://doi.org/10.1182/blood-2010-01-263145
29. Choi C, Benveniste EN. Fas ligand/Fas system in the brain: regulator of immune and apoptotic responses. Brain Res Rev. 2004;44(1):65–81. https://doi.org/10.1016/j.brainresrev.2003.08.007
30. Hosseinalizadeh H, Rabiee F, Eghbalifard N, Rajabi H, Klionsky DJ, Rezaee A. Regulating regulatory T cells as cell therapies in autoimmunity and cancer. Front Med. 2023;10:1244298. https://doi.org/10.3389/fmed.2023.1244298
31. Fernald GH, Capriotti E, Daneshjou R, Karczewski KJ, Altman RB. Bioinformatics challenges for personalized medicine. Bioinformatics.2011;27(13):1741–1748. https://doi.org/10.1093/bioinformatics/btr295